UPPSALA
UNIVERSITET

Multiscale methods for porous media flow problems

Fredrik Fernlund
Jon Hassis
Ossian O'Reilly
Supervisor: Axel Målqvist
Department of Scientific Computing

2010-06-02

Abstract

We make a quality analysis of the multiscale finite element method (MsFEM) when solving the pressure equation for flows in porous media that contains a multiscale structure. This analysis is done by considering the ordinary finite element method as the reference solution.

It has been suggested that the MsFEM can capture the small scale information and transport it to the large scale so that the computational cost can be reduced. In this report, we compare the methods for different types of permeability structures, since it has been proposed that the MsFEM will render inaccurate solutions for channelized permeability structures. We show that, indeed, the MsFEM seems to give undesirable results for media containing canals.

Keywords: Multiscale finite element method, Random perturbation, Darcy's law, Oil reservoir simulation, Groundwater flow.

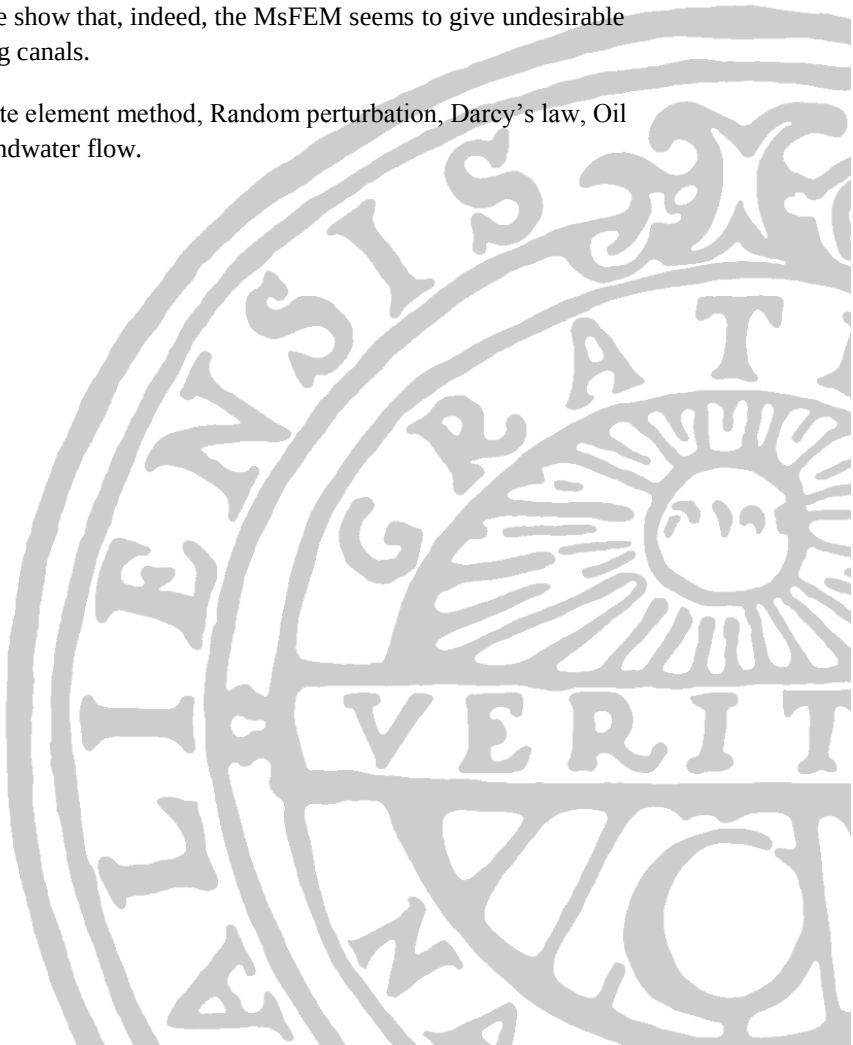

Contents

1. Introduction

There are many engineering applications that are of practical importance with multiscale behaviour. Multiscale problems include for example problems of porous media, composite materials and turbulent transport flows. It is very difficult to do a complete analysis of these problems with standard one mesh methods since there is heterogeneity in many scales. In groundwater flow heterogeneity is present due to fluctuations in permeability. The permeability is a measurement of the ability of a porous medium to transmit fluids (often denoted κ or k and the SI unit is m^2). Figure 1 shows the permeability in an oil reservoir where we can see a distinct canal.

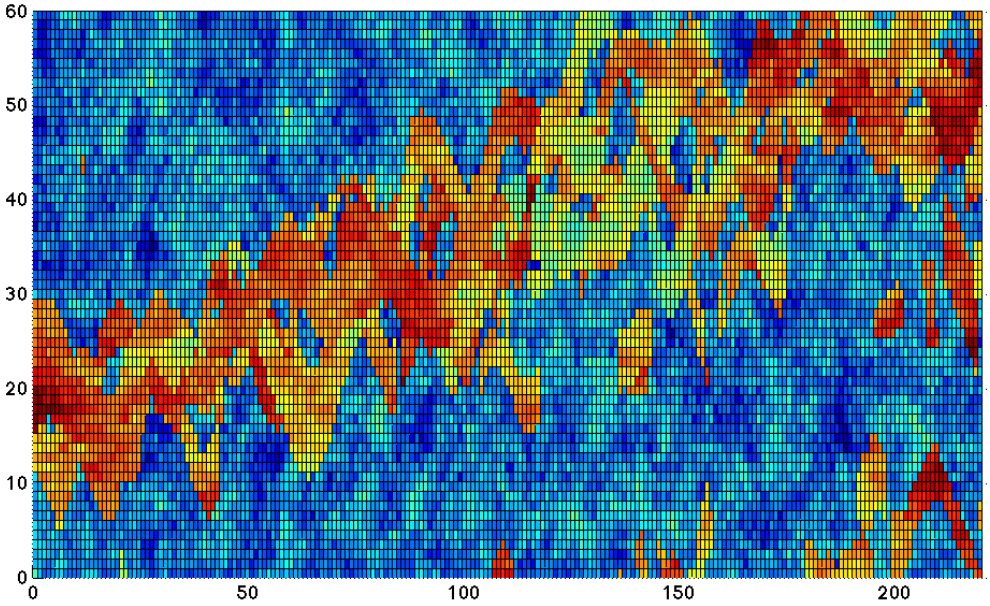

Figure 1: The permeability in an oil reservoir.

One can find several cases in earth science with flow through porous media where permeability has to be considered. For example carbon dioxide capturing, groundwater flow and flow in an oil reservoir. When using conventional numerical methods the multiscale problem requires a lot of CPU time and memory, since the mesh needs to be highly resolved. Therefore, it is desirable to use a numerical method that captures the small scale effects on the large scale but does not require resolving all the small scale features globally; this is the purpose of the multiscale method.

Previous work. During the last two decades, a lot of research in multiscale methods has been done. One of these methods is called the Multiscale Finite Element Method (MsFEM) and was developed by Hou and Wu [1]. The method relies on homogenization theory to construct modified finite element method (FEM) basis functions which capture fine structures. Målqvist and Larson propose another

multiscale method [2] which is a new adaptive multiscale finite element method. In [2] they also derive an a posteriori error estimate in terms of the energy norm.

New contributions. In this report we examine the quality of MsFEM by using the relative energy norm with ordinary FEM as the reference solution. We also compare the methods by tracing individual particles in the velocity field produced from Darcy's law, and keeping track of the time it takes them to travel a certain distance. Once again, the FEM is considered as a reference.

Outline. In section 2 the physical background for multiscale problems is presented. In section 3 is a brief explanation of the theory behind FEM and MsFEM described. In section 4, the numerical results are presented. In section 5, the conclusions and in section 6 is the discussion. In section 7 are the references presented and section 8 contains the appendix.

2. Physical problems

2.1 Groundwater flow

In hydrology, the groundwater flow equation is often used show the mathematical relationship which describes the flow of water through an aquifer. An aquifer is an underground layer of unconsolidated materials, for example sand or clay. We derive the groundwater flow equation by considering the conservation of mass. Since mass cannot be destroyed, nor be created, aside from sources and sinks. Then for a given increment in time (Δt), the difference between the mass flowing in at the boundaries, the mass flowing out at the boundaries and the sources in the volume, is the change in storage volume.

$$\frac{\Delta M_{storage}}{\Delta t} = \frac{\Delta M_{in}}{\Delta t} - \frac{\Delta M_{out}}{\Delta t} - \frac{\Delta M_{generated}}{\Delta t} \qquad (1)$$

We express the mass in terms of density and volume and assume incompressible flow. Furthermore we consider Taylor series and the divergence theorem. Finally we obtain the differential form of the transient groundwater flow equation.

$$S_s \frac{\partial h}{\partial t} = -\nabla \cdot q - G \qquad (2)$$

(2) states that the change in hydraulic head (h) with respect to time (LHS) is equal to the negative divergence of the flux of the whole volume (q) and the source term (G). The hydraulic head is a measurement of water pressure above a given reference point.

A very important equation in the study of flow through porous media is Darcy's law. Darcy's law is a simple relationship between the instantaneous flow rate through a porous medium, the viscosity and the pressure gradient.

$$q = \frac{-\kappa}{\mu}\nabla P \quad (3)$$

where q is the discharge per unit area, with units of length per time m/s, ∇P is the pressure gradient. κ is the permeability of the medium and μ is the dynamic viscosity.

By using (3), one can relate the flux (q) with hydraulic heads which leads to

$$S_s \frac{\partial h}{\partial t} = -\nabla \cdot (\kappa \nabla h) - G \quad (4)$$

which is the final form of the groundwater flow equation.

2.2 Flow in oil reservoir

An oil reservoir is a pool of hydrocarbons contained in a porous medium such as a rock formation. The hydrocarbons that are of interest are trapped by overlying rock formations with lower permeability. One way to produce oil from the reservoirs is to inject water into the reservoir in one end and then extract the oil from another end of the reservoir. When injecting the water, the pressure increases and that stimulates the production. This process is shown in figure 2 below.

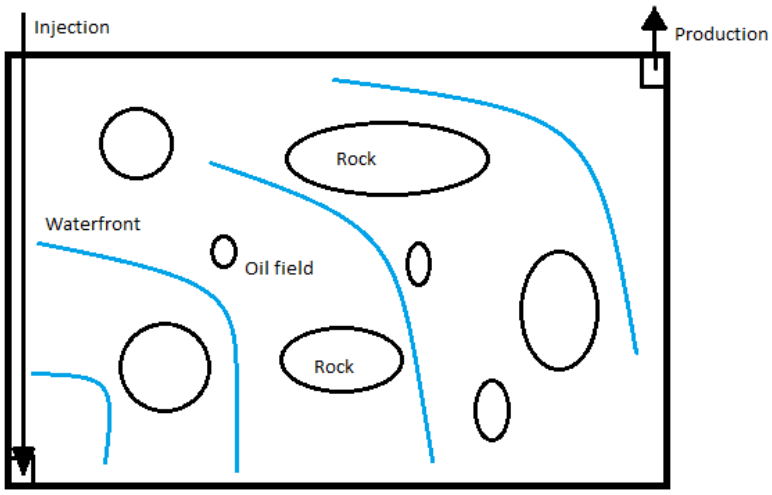

Figure 2: The process of oil production when injecting water.

To describe the motion of a fluid in an oil reservoir one must state some things first.

We consider two-phase flow under the assumption that the displacement is dominated by viscous effects, neglecting the gravity, compressibility and capillary pressure.

By using a similar mass conservation discussion as in the groundwater flow section, we can state the following equation.

$$\rho \nabla \cdot q - Q = 0 \quad (5)$$

Here ρ is the density, q is the flux of the fluid and Q is some source or sink term. We combine Darcy's law with (5) and finally get a simplified version of the pressure equation.

$$-\nabla \cdot \left(\frac{\kappa}{\mu}\nabla P\right) = \frac{Q}{\rho} \qquad (6)$$

If we consider the saturation of water in the oil reservoir the pressure equation reads

$$-\nabla \cdot (\lambda(S)\kappa\nabla P) = \frac{Q}{\rho} \qquad (7)$$

where S is the concentration of water and λ is the total mobility, given by

$$\lambda(S) = \frac{\kappa_{rw}(S)}{\mu_w} + \frac{\kappa_{ro}(S)}{\mu_o} \qquad (8)$$

In (8), the subscripts w and o denotes water and oil respectively. Now we state the so-called pressure and saturation equations

$$-\nabla \cdot (\lambda(S)\kappa\nabla P) = \frac{Q}{\rho}$$

$$\frac{\partial S}{\partial t} + v \cdot \nabla b(S) = 0 \qquad (9)$$

where λ is the total mobility, κ is the permeability tensor, P is the pressure and Q is a source/sink term; S is the concentration of water and v is the velocity in m/s, obtained from Darcy's law. These equations are computationally demanding to solve because of the coupling through the concentration of water.

2.3 Carbon dioxide capturing

Carbon capture and storage (CCS) is a method employed to reduce the intensity of carbon dioxide in the atmosphere. It works by injecting carbon dioxide directly into geological formations. Proposed injection sites include oil fields, gas fields and unminable coal seams. Carbon dioxide is also sometimes injected to declining oil fields to increase oil recovery. The governing equations for injection of carbon dioxide into geological formations are the same as the flow in an oil reservoir discussed earlier.

3. Description of problems

3.1 Problem formulation

In our problem we are going to solve (7) for the pressure, assuming $\lambda = 1$ for simplicity. This will be done both with MsFEM and FEM, where FEM will be used as a reference solution.

Once again, the governing equations are:

$$\begin{cases} -\nabla \cdot (\lambda(s)\kappa \nabla P) = \frac{Q}{\rho} \\ \frac{\partial S}{\partial t} + v \cdot \nabla b(S) = 0 \end{cases}, \ (x, y) \in \Omega \qquad (10)$$

The domain Ω is defined by the physical rectangular domain [2200x1200] (ft)

We consider no externally applied pressure on the boundary, so that our boundary conditions are Neumann

$$n \cdot \nabla P|_{\partial\Omega} = 0 \qquad (11)$$

where n is the unit normal vector to the boundary.

We will only consider the steady state solution of (10) so we will ignore the saturation equation.

Since we want to simulate a change in pressure that will create a flow across the domain we introduce a source and sink a term Q_+ and Q_-.We set the source term $Q_+ = 1$ in the lower left corner and the sink term $Q_- = -1$ in the upper right corner, and $Q = 0$ everywhere else on the domain. To simplify the notation we introduce the source/sink function $f(x, y)$

$$f(x, y) = \begin{cases} 1, & (x, y) \in \text{lower left corner} \\ -1, & (x, y) \in \text{upper right corner} \\ 0, & \text{else where} \end{cases}$$

where f satisfy the condition $\iint_\Omega f(x, y)dxdy = 0$, which is needed for a solution to exist. We also assume $\rho = 1$. As usual κ is the permeability tensor and P is the pressure. The choice of the source/sink term will simulate a pressure difference which will create a flow in the domain. Then equation (10), (11) becomes

$$\begin{cases} -\nabla \cdot (\kappa \nabla P) = f \\ n \cdot \nabla P|_{\partial\Omega} = 0 \end{cases}, \ (x, y) \in \Omega \qquad (12)$$

The values of κ being chosen from a layer in a three dimensional matrix, representing the permeability in a rectilinear block. Each layer contains 220 x 60 elements. We will consider the permeability to be isotropic in x and y directions for each of the layers. The permeability matrices used, comes from the tenth SPE comparative solution project*.

Below, in figure 3, is a graphical illustration of layer 76 in the three dimensional matrix we will study.

---

* http://www.spe.org/web/csp/datasets/set02.html

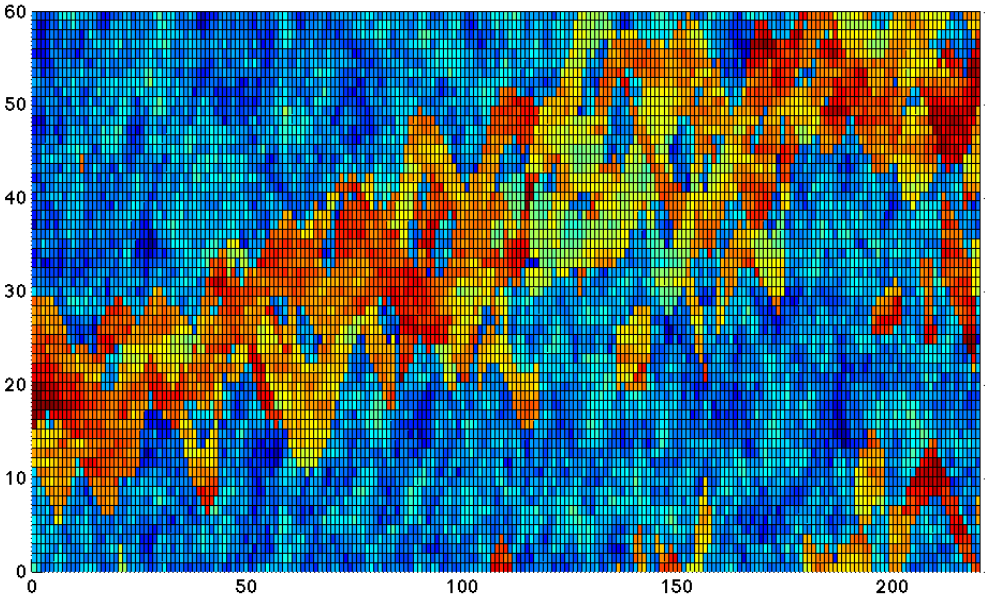

Figure 3: Permeability matrix for layer 76.

In figure 3, the red areas show where water easily can penetrate and we see that this layer contains a distinct canal.

3.1.1 The Finite element method

We now start deriving the finite element method for solving (12). First we will find the weak formulation of (12) and then we will introduce the finite element approximation and choose a suitable basis.

The weak formulation is obtained by taking any test function v where $v \in V$. Where the space V is defined as

$$V = \{v: \|\nabla v\| + \|v\| < \infty\} \qquad (13)$$

Then if we multiply (12) with any test function $v \in V$ we get

$$-\nabla \cdot (\kappa \nabla P)v = fv, \quad \forall v \in V \qquad (14)$$

Now integrate over the entire domain Ω

$$\iint_{\Omega} -\nabla \cdot (\kappa \nabla P)v \, dA = \iint_{\Omega} fv \, dA, \quad \forall v \in V \qquad (15)$$

We use Green's theorem and the boundary condition (11). Finally, we obtain the weak form to (12): Find $P \in V$ such that:

$$\iint_\Omega \kappa \nabla P \cdot \nabla v \, d\mathrm{A} = \iint_\Omega f v \, dA, \quad \forall v \in V \qquad (16)$$

Furthermore, we introduce the finite element approximation. Let V_h be the space of continuous and piecewise bilinear functions defined on the quadrilateral partitioning of Ω. Then the finite element formulation becomes

Find $U \in V_h$ such that:

$$\iint_\Omega \kappa \nabla \mathrm{U} \cdot \nabla v \, d\mathrm{A} = \iint_\Omega f v \, dA, \quad \forall v \in V_h \qquad (17)$$

Furthermore, let $\{\Phi_i\}_{i=1}^N$ be a basis in V_h, that is,

$$\Phi_\mathrm{i}(N_j) = \begin{cases} 1, & i = j \\ 0, & i \neq j \end{cases} \qquad (18)$$

where N_j is a node on the mesh and N is the number of nodes on the mesh. Then we can write U in the following way

$$U = \sum_{i=1}^N \alpha_i \Phi_i \qquad (19)$$

So that the problem becomes, find α_i, such that:

$$\iint_\Omega \kappa \alpha_i \nabla \Phi_i \cdot \nabla \Phi_j \, d\mathrm{A} = \iint_\Omega f \Phi_j \, dA, \quad i,j = 1,2,\ldots,N \qquad (20)$$

In our case we will only consider piecewise bilinear basis functions as stated earlier. However it is possible to construct basis functions of higher order.

Since Ω is a rectangular domain it is easy to generate a mesh of Ω using rectangular elements. We let $\mathcal{Q}$ denote the rectangular equidistant discretization of Ω. Let h_x , h_y be the spatial lengths defined by

$$h_x = \frac{2200}{N_x} \qquad (21)$$

$$h_y = \frac{1200}{N_y} \qquad (22)$$

where N_x, N_y is the number of nodes along the x-scale and y-scale respectively. Then on every rectangular element Q_k of Ω we construct bilinear basis functions Φ_i .

Each basis function Φ_i can be uniquely determined, using the following ansatz and the properties of the basis functions (18):

$$\Phi_\mathrm{i}(x,y) = \mathrm{ax} + \mathrm{by} + \mathrm{cxy} + \mathrm{d} \qquad (23)$$

On Q_k this is a linear system of equations with unknowns a, b, c and d. Solving (23) for each node in the rectangle yields the following basis functions with the coordinate system defined as in figure 4.

$$\Phi_1(x,y) = \frac{(h_x - x)(h_y - y)}{h_x h_y} \qquad (24)$$

$$\Phi_2(x,y) = \frac{x(h_y - y)}{h_x h_y} \qquad (25)$$

$$\Phi_3(x,y) = \frac{xy}{h_x h_y} \qquad (26)$$

$$\Phi_4(x,y) = \frac{(h_x - x)y}{h_x h_y} \qquad (27)$$

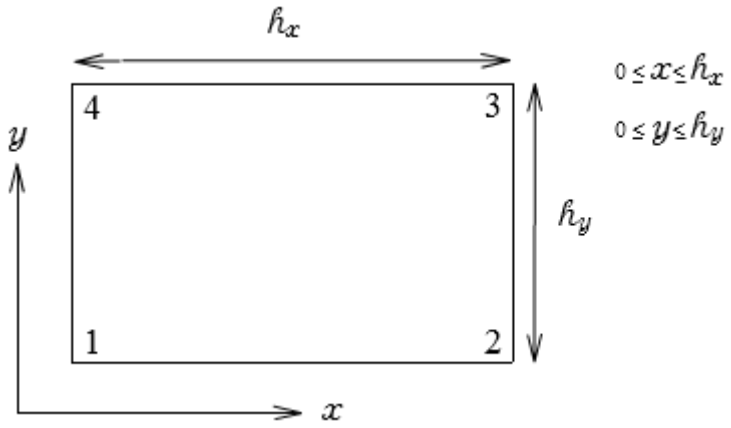

Figure 4: Rectangular element, 1 – 4 indicate nodal points.

Once we have defined our basis functions on each rectangular element Q_k we get the linear system of equations

$$\sum_{j=1}^{N} \alpha_i \iint_{\Omega} \left(\kappa \nabla \Phi_i \cdot \nabla \Phi_j\right) dx\mathrm{d}y = \iint_{\Omega} f \Phi_i \, dxdy \quad i = 1,2,\dots,N \qquad (28)$$

where the integrals can be rewritten as a sum over all elements, Q_k, and computed exactly for bilinear functions.

3.1.2 The Multiscale Finite Element Method

The main idea behind MsFEM is to incorporate the small scale structure into finite element basis functions and capture their effect on the large scale by finite element computations. This is done using homogenization theory since then the fine scale problem can be decoupled into several fine scale problems. Each fine scale problem can then be solved to construct coarse scale basis functions which capture the fine scale structure.

The domain Ω is subdivided into macro scale elements called the coarse scale, where each macro scale element is subdivided into micro scale elements called the fine scale, see figure 5. Each micro scale

element corresponds to one element of the permeability matrix. The number of elements of the permeability matrix is always fixed which limits the number of possible MsFEM resolutions. (In the results section we will examine the impact of the accuracy for a chosen number of MsFEM resolutions.)

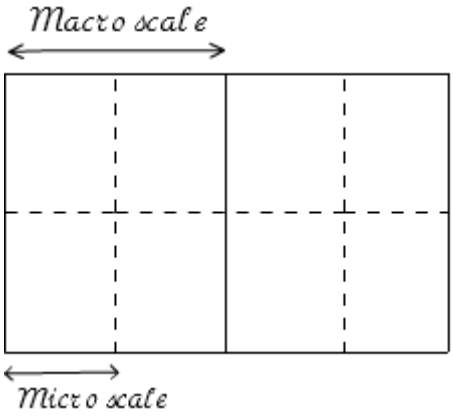

Figure 5: Macro scale elements and 2x4 micro scale elements.

MsFEM uses modified basis functions to construct the solution on the coarse scale. The modified basis functions can be viewed as the ordinary bilinear basis functions with a fine structure which has captured the fine scale variations. The basis functions are constructed by solving a homogenized problem on the fine scale with the permeability taken into account. When we construct the MsFEM basis functions Φ_i we consider a superposition of bilinear basis functions φ_j

$$\Phi_i = \sum_{j=1}^{n} \beta_j \varphi_j \qquad (29)$$

where n is the number of elements on the fine scale of a macro element.

Then we seek to solve the homogenized problem on every macro scale element Q_k of Ω.

$$-\nabla \cdot \left(\kappa \nabla \Phi_{i,k}\right) = 0, \ (x, y) \in Q_k \qquad (30)$$

with boundary conditions

$$\Phi_{i,k}\big|_{\partial\Omega} = g_i \qquad (31)$$

where the choice of g_i will be described below.

By choosing a test space, V_0, with functions that are zero on the boundaries the boundary term in the weak form

$$\iint_{\Omega} \kappa \nabla \Phi \cdot \nabla v \, dA - \int_{\partial\Omega} n \cdot \kappa \nabla \Phi v \, dS = 0, \ \forall v \in V_0 \qquad (32)$$

will disappear and the finite element approximation becomes, find $U \in V_{h,0}$ such that:

$$\iint_{\Omega} \kappa \nabla U \cdot \nabla v \, dA = 0, \quad \forall v \in V_{h,0} \qquad (33)$$

$$U(x_j) = g(x_j)$$

where x_j are the boundary nodes.

Setting

$$U = \sum_{i=1}^{N} \beta_i \varphi_i \qquad (34)$$

and noting that $V_{h,0}$is spanned by the interior basis functions φ_i for $i = 1{:}\, N,$ we get the linear system of equations:

$$\iint_{\Omega} \kappa \beta_i \nabla \varphi_i \cdot \nabla \varphi_j \, dA = 0 \quad \forall \varphi_i, \ \varphi_j \in V_h, \ i, j = 1,2,\ldots,N, k = 1,2,3,4 \quad (35)$$

We will solve (35) for the unknown coefficients β_i four times on every macro element but with different boundary conditions since there are four macro scale basis functions on every macro scale element.

Since the permeability is only known in the interior region of each macro element we must take special care of how we treat the boundary term. If the permeability is sampled directly from the interior region discontinuous basis functions will arise. To avoid discontinuous basis functions we will instead impose linear behaviour on the boundary. Figure 7 shows one of the solutions to (35) where linear boundary conditions has been used.

Another approach is to sample the average permeability for neighboring regions, see figure 6, and solving the corresponding one dimensional equations

$$\frac{d(\kappa \Phi_i)}{dx} = 0 \quad \text{and} \quad \frac{d(\kappa \Phi_i)}{dy} = 0 \qquad (36)$$

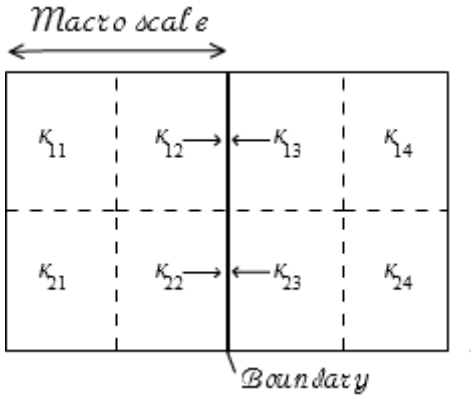

Figure 6: Averaging the permeability across the boundaries to avoid discontinuous basis functions.

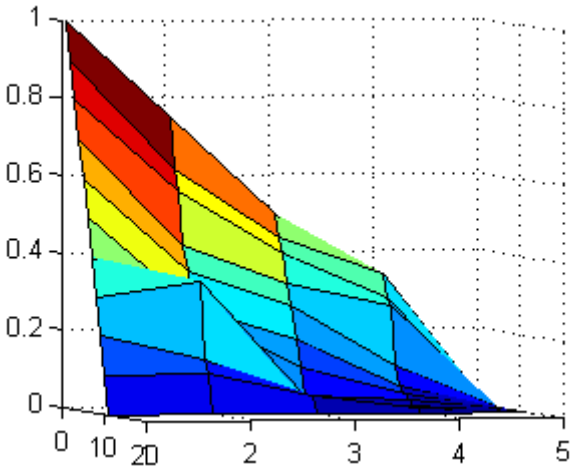

Figure 7: Small scale features captured by partial MsFEM basis function with linear boundary edges

Once we have computed the modified basis functions Φ_i by determining the coefficients β_i on all macro scale elements we need to solve the inhomogeneous problem on the coarse scale using the modified basis functions as our basis.

We now show how to solve the coarse scale problem using the modified basis functions. We assume that the coefficients β_i of every modified basis function are known so that all modified basis functions has been determined. Then we want to find the solution on the coarse scale in terms of the unknown coefficients α_i. We formulate the Multiscale finite element method by seeking the solution to the weak form in the space spanned by the Multiscale finite element basis functions. This leads to the following system of equations:

$$\sum_{j=1}^{N} \alpha_i \iint_{\Omega} \beta_i \sum_{l=1}^{n} \nabla\varphi_l \cdot \beta_j \sum_{l=1}^{n} \nabla\varphi_l \, dxdy = \iint_{\Omega} f\beta_i \sum_{l=1}^{n} \varphi_l \, dxdy \quad i = 1{:}N \qquad (36)$$

where the gradients are approximated with its value at the center of each fine scale element.

3.2 Analysis and evaluation

When examining the multiscale finite element method, it is important to look at different types of global scale permeabilities. This is because when using the MsFEM, one decouples the problem on coarse elements and it is then crucial that the differential operator behaves locally. When the porous media contains canals, this prerequisite is violated, and the method is expected to be inaccurate [4].

3.2.1 Energy norms

One way to evaluate the quality of the MsFEM is to use the energy norm with ordinary FEM (220x60 elements) as the reference solution, i.e:

$$\left\| \sqrt{\kappa} \nabla (P_{MsFEM} - P_{FEM}) \right\|_{\Omega} \qquad (37)$$

where we have approximated the gradients with the midpoint value of each element.

To be able to compare the obtained results we compute the relative energy norm, i.e:

$$\frac{\left\| \sqrt{\kappa} \nabla (P_{MsFEM} - P_{FEM}) \right\|_{\Omega}}{\left\| \sqrt{\kappa} \nabla P_{FEM} \right\|_{\Omega}} \qquad (38)$$

We compute the relative energy norm for all layers and a handful of partitions.

3.2.2 Statistical analysis of the time from injection to extraction

When the pressure is obtained, one can, using Darcy's law, calculate a velocity field in the domain. This can then be used to simulate individual particles travelling through the medium, by assigning it a velocity corresponding to its location and step with an appropriate finite difference method. By using a large number of particles and investigating the time it takes for one of them to get from the inlet to the outlet, one can compare the multiscale method with ordinary FEM.

The analysis is done by doing a large number of the tests described above with different permeabilities, each permeability being constructed by adding a random noise to the original permeability. Since the measurements of the permeability are associated with errors it is of interest to see how sensitive the solution is to random perturbations in the permeability. We choose to examine two different layers, one where the permeability is fairly evenly distributed and one where there is a distinct canal. Each of these layers is perturbed 4000 times where the size of the perturbation is chosen from a uniform random distribution with max and min values of +/-20% of the elements original value.

By doing tests with both FEM and MsFEM with the same 4000 different permeabilities, one obtains a cumulative distribution function for each method which can be analyzed and compared.

A direct consequence of the central limit theorem is that

$$|F_n(t) - F(t)| < \gamma\sqrt{\frac{|F(t)*(1-F(t))|}{n}} \qquad (39)$$

where $F_n(t)$ is the empirical cumulative distribution function (CDF) and $F(t)$is the true CDF (n=∞). Using γ =2,58 for a 99% confidence interval and with 0.25 as an upper bound for $|F(t) * (1 - F(t))|$, our n =4000 times yields $|F_n(t) - F(t)| < 0{,}02$. If the difference $|F_{FEM}(t) - F_{MsFEM}(t)| \gg 0{,}02$ one can be reasonably sure that an observed difference between the methods will not depend on a statistical error.

4. Numerical results

4.1 Pressure fields

First, we implement both FEM and MsFEM to solve eq. 11 for the pressure, the FEM solution being intended to use as a reference. Figure 8 shows the FEM solution for permeability layer 85 and we clearly observe all small scale details.

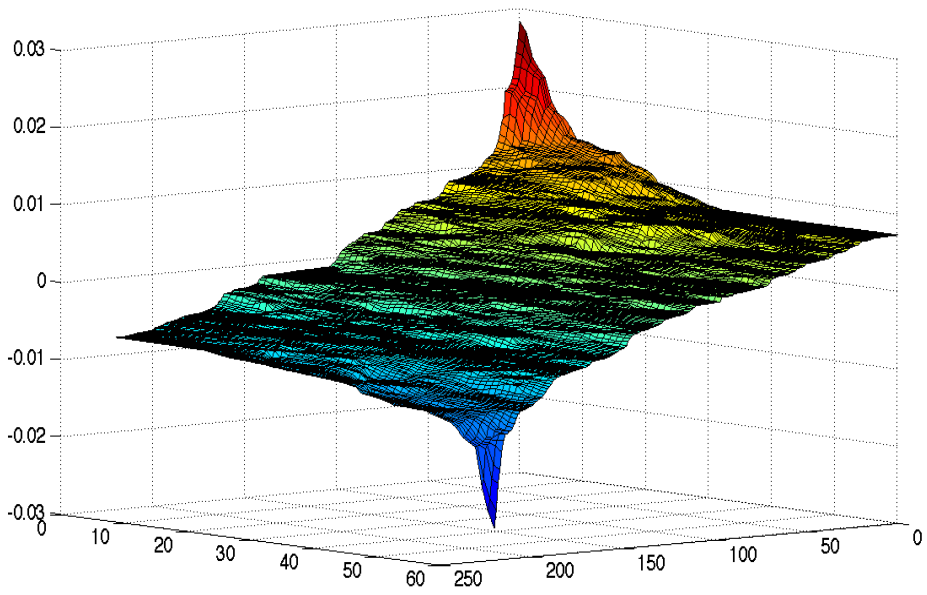

Figure 8: Solution of the pressure for layer number 85

In figure 9, an MsFEM solution with a partitioning of 55x30 macro elements as well as 22x15 are shown.

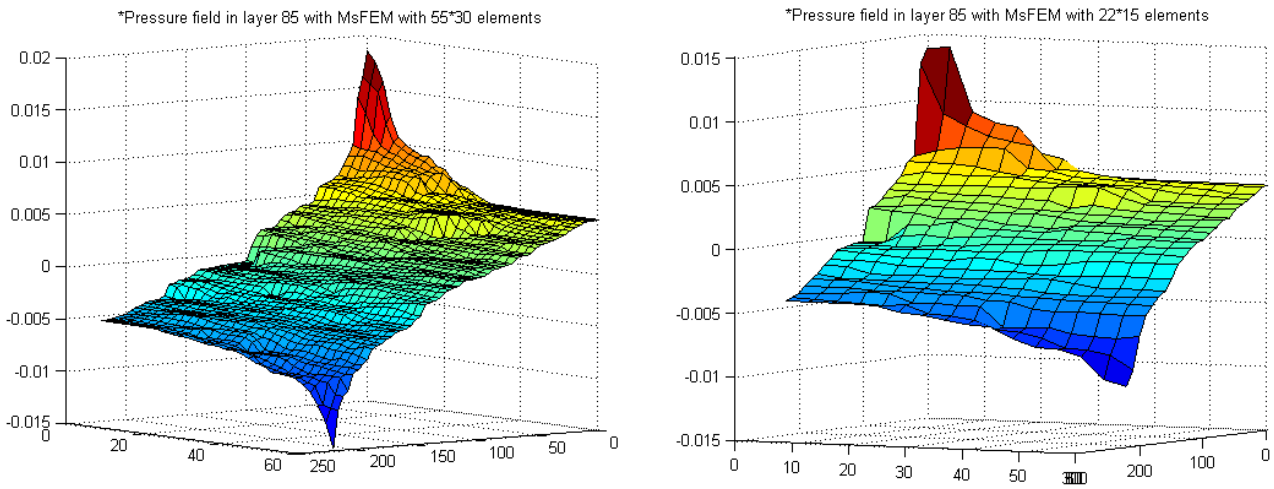

Figure 9: Solution of the pressure with MsFEM for layer number 85. Partitioning of 55x30 elements (left), partitioning of 22x15 (right).

We see that we lose some details on the fine scale when increasing the partitioning. The observant reader also notes that the solutions max and min value differ, FEM having about 0.03, MsFEM 55x30 about 0.02 and MsFEM 22x15 about 0.015. This will substantially affect the gradients which in turn affect the velocity fields.

When inspecting layer 60 with both FEM and MsFEM, we get solutions as in figure 10.

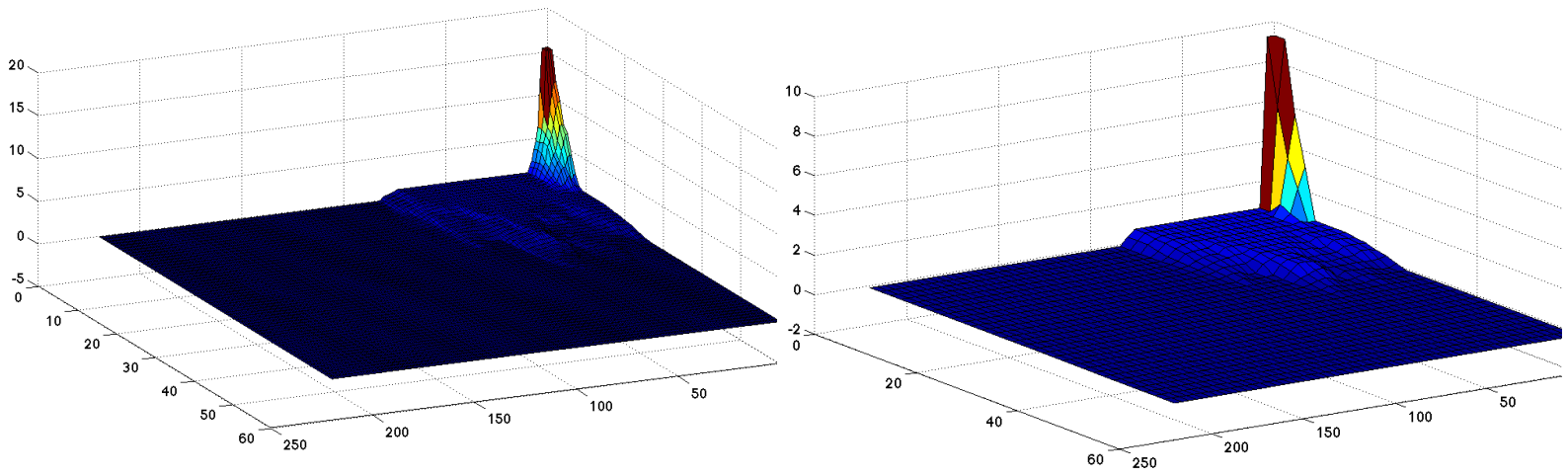

Figure 10: Solution of the pressure with FEM for layer number 60 (left). Solution of the pressure with MsFEM 55x30 (right).

The solution of the pressure for layer 60 with a partitioning of 55x30 is shown to the right in figure 10 and we can see that the tendency to reduce the overall pressure, compared to the FEM solution, is present also in this case.

4.2 Energy norms

We are interested in examining the energy norm in all layers and for a handful of different partitions. In figure 11, we have chosen five different partitions and plotted the relative energy norms for all layers.

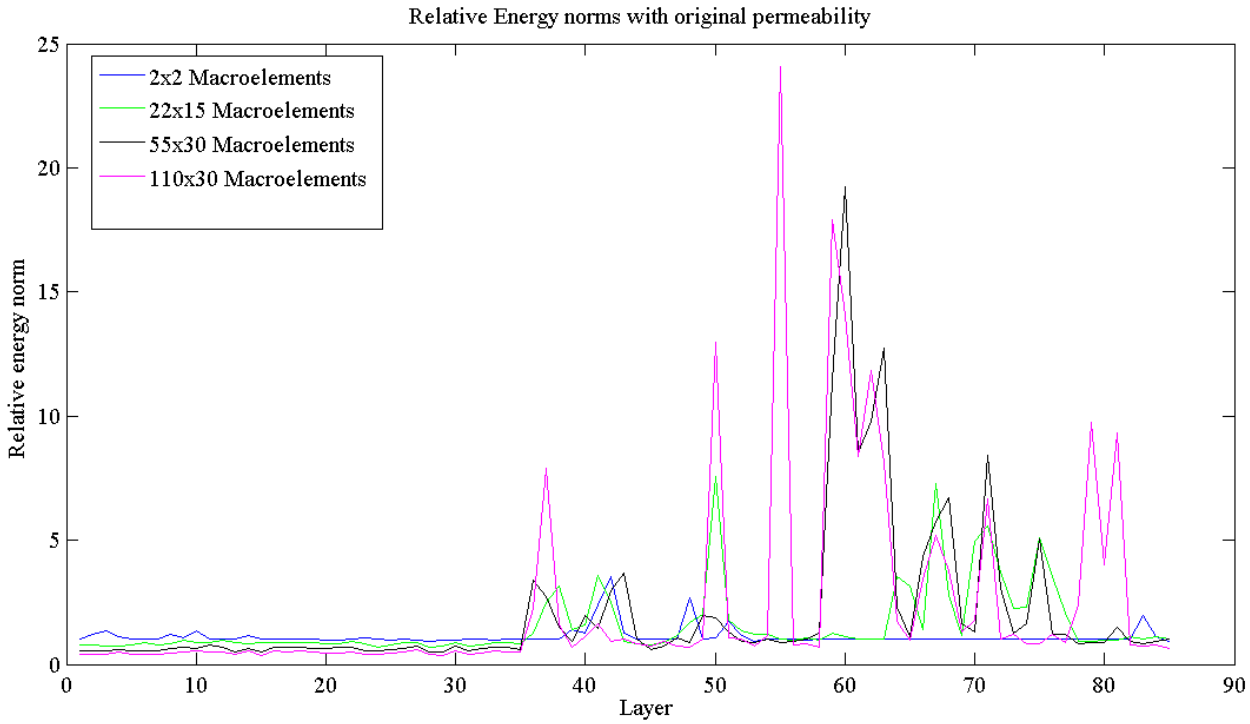

Figure 11: Energy norms with layers on the x-axis and different partitions

An observation of figure 11 reveals that at layer 35 the relative energy norms start to increase rapidly. This is probably due to nature of those layers, a possible explanation as to why this is, can be given in figure 12, where a graphical logarithmic representation of the permeability structures in layer 1 and 60 are depicted. As mentioned in section 4.2, it is expected that the MsFEM is inaccurate in permeability structures containing canals. Examining figure 12, we can see that layer 60 has a distinct canal whereas in layer 1, the permeability is much more evenly distributed. This means that the expectation that MsFEM is inaccurate in the presence of canals seem to be fulfilled.

We notice that the energy norm for the partition 2x2 is rather evenly distributed for all layers and among the 30 last layers it is best in terms of the relative energy norms. This further illuminates the extreme poorness of MsFEM in those layers.

In table 1 in the appendix, the energy norms for all of the 11 partitions are shown.

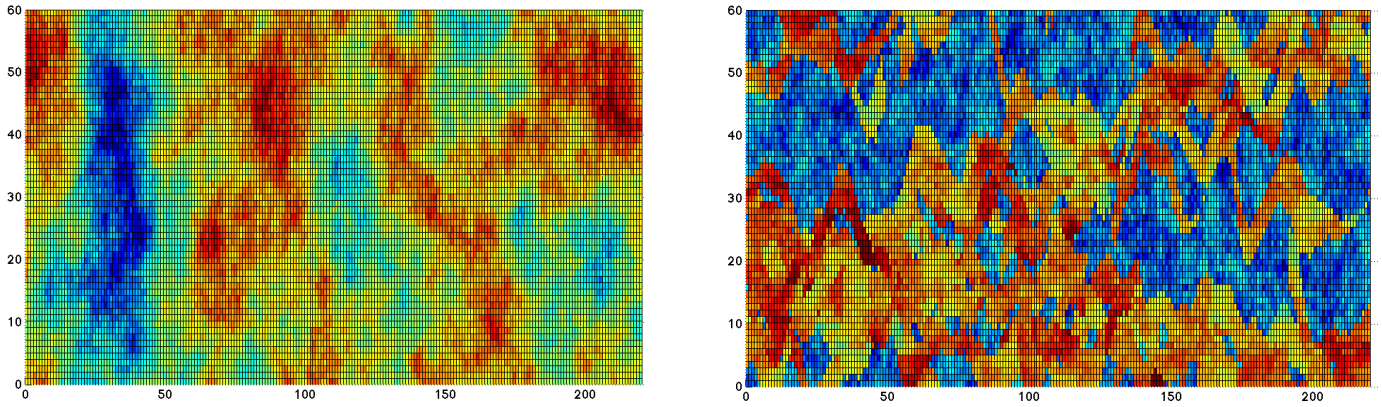

Figure 12: Graphical logarithmic representation of the permeability in layer 1 (left) and layer 60 (right).

4.3 Analysis of breakthrough times

As mentioned before, in section 3.2, we are, as a comparison between FEM and MsFEM, interested in tracing the motion of individual particles through the medium and, especially, the time it takes them to get from the inlet to the outlet.

Shown below, in figure 13, is the results of an simulation of the trajectories of 1500 particles whose velocities are taken from the vector field obtained by Darcy's law. The particles initial positions were evenly distributed on a quarter circle in the lower left corner and the time was stopped when the first particle reached the red circle in the upper right corner.

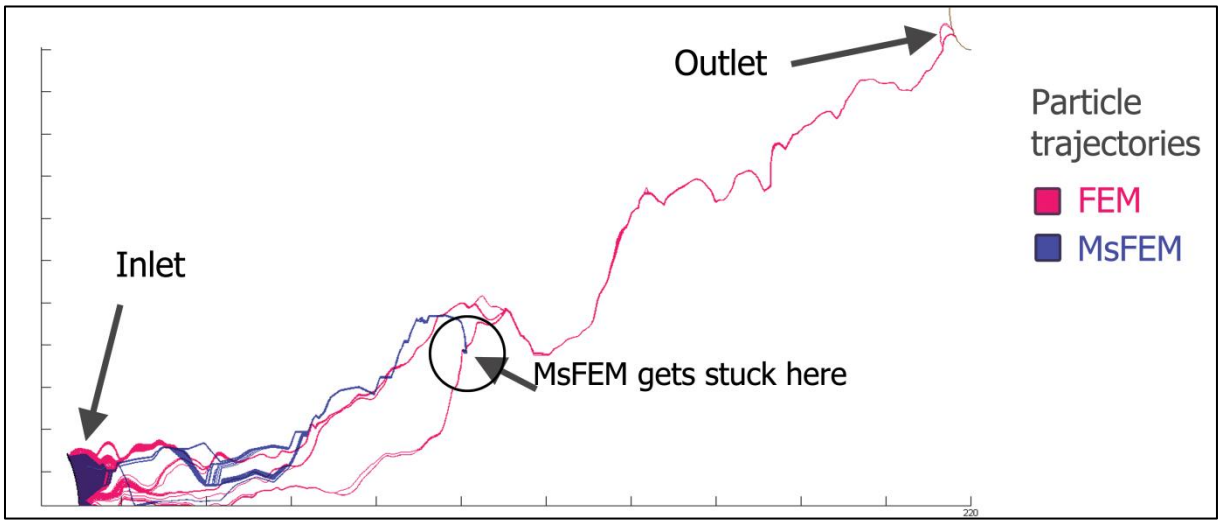

Figure 13: Trajectories for both MsFEM 55x30 and FEM for layer 76.

Figure 13 depicts the situation in layer 76, which contains a canal. Also here, we see that MsFEM fails to give a desirable result.

4.3.1 Statistical analysis

Shown below, are the results from the statistical analysis described in section 4.2. At first we examine layer 1, which is one the layers that doesn't contain a canal. In figure 14, the empirical CDF:s for FEM and MsFEM 55x30 are shown. Although this layer has a fairly evenly distributed permeability, we see that there is a clear difference between the methods.

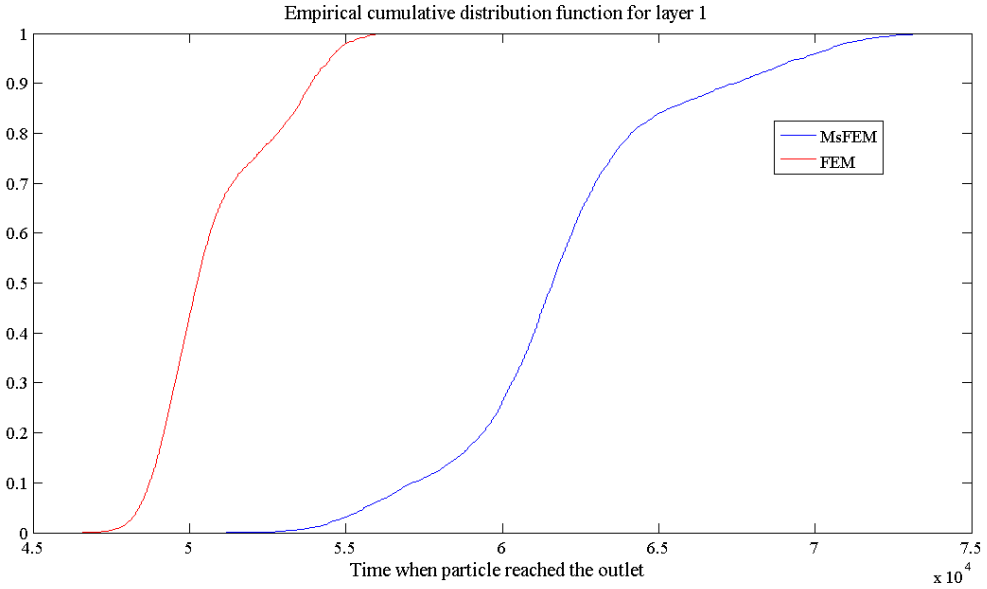

Figure 14: Empirical distribution functions for layer 1

In figure 15, the difference between the red and the blue line in figure 14 are shown. As we described in section 4.2, we want this difference to be much larger than 0,02. For 80% of the particles it is larger than 0,2 i.e. 10 times larger than 0,02. This leads us to the conclusion that the difference between the CDF:s lies in the difference of the methods and not in a statistical error.

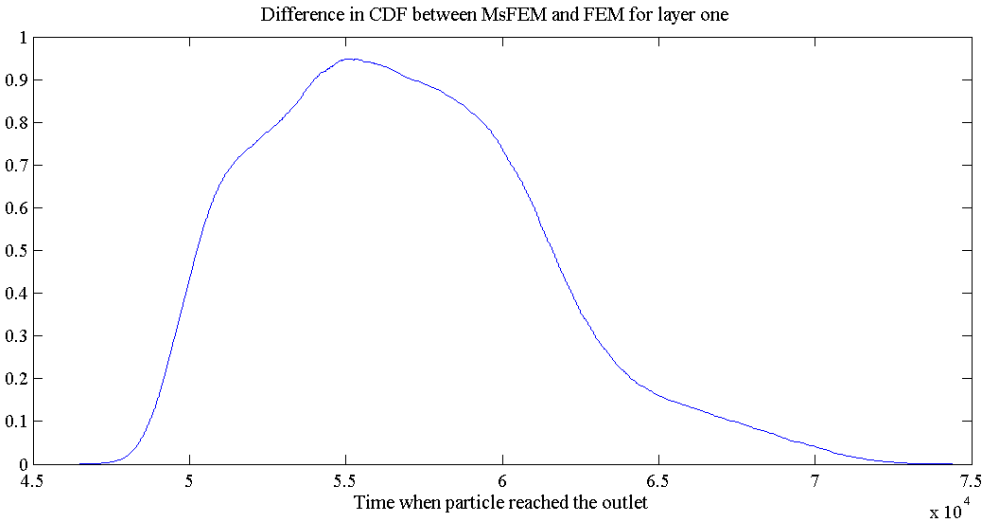

Figure 15: Difference between empirical CDF:s of MsFEM and FEM for layer 1

In figure 16 the empirical probability densities for MsFEM and FEM in layer 1 are shown. This figure clearly illustrates that MsFEM gives a displacement of the mean value as well as a larger spread in the data compared to FEM.

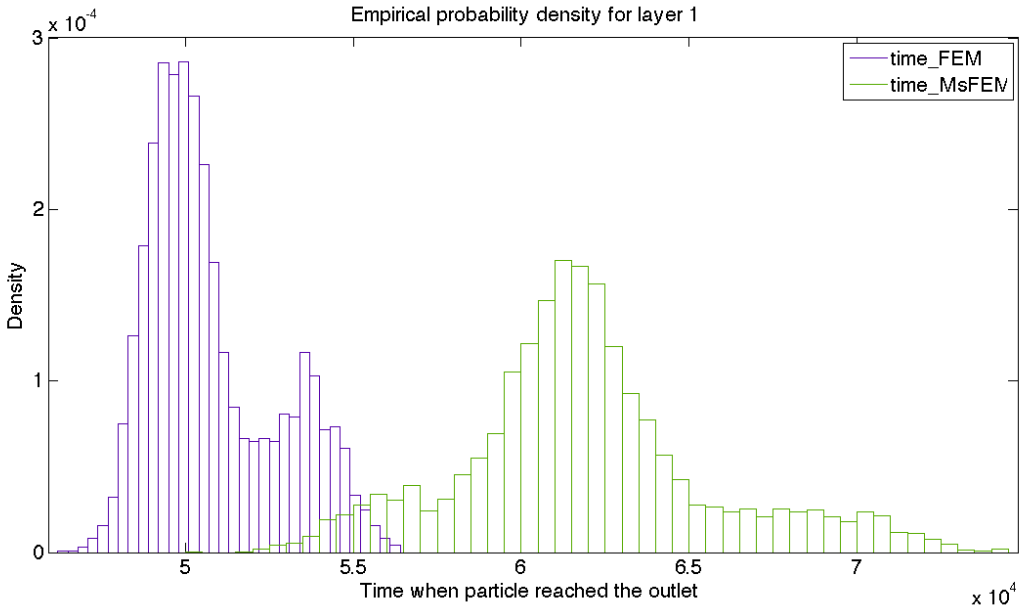

Figure 16: Empirical probability densities for layer 1.

Now we examine layer 60 in the permeability matrix, which is a layer that contains a distinct canal (see figure 12). In figure 17, the empirical CDF:s for FEM and MsFEM 55x30 are shown. If we compare this figure to the one for layer 1, we notice that this distribution is more displaced than the previously as well as more spread

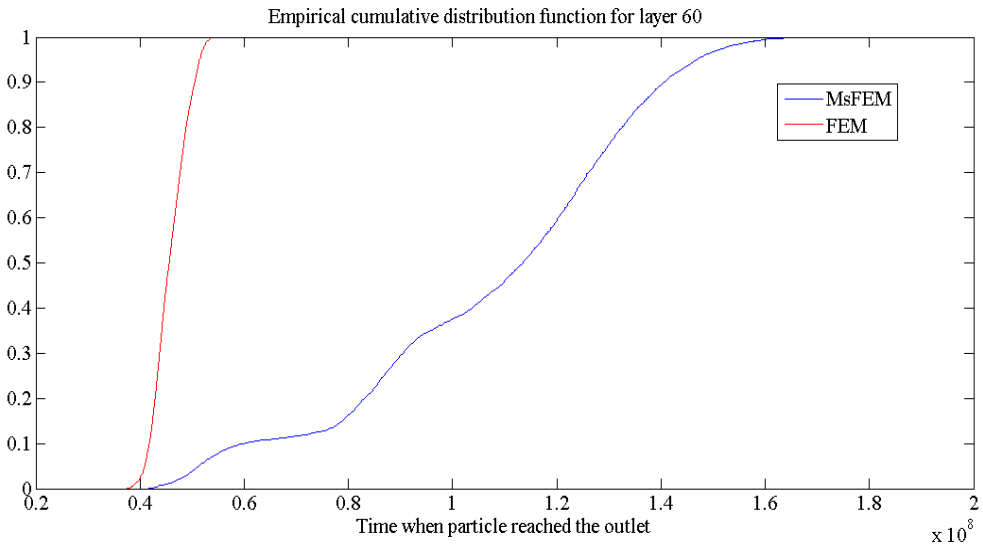

Figure 17: Empirical distribution functions for layer 60

In figure 18, the difference between the red and the blue line in figure 17 are shown. Also here we notice that the difference is much larger than 0,02 which tells us once again that the error is of numerical type.

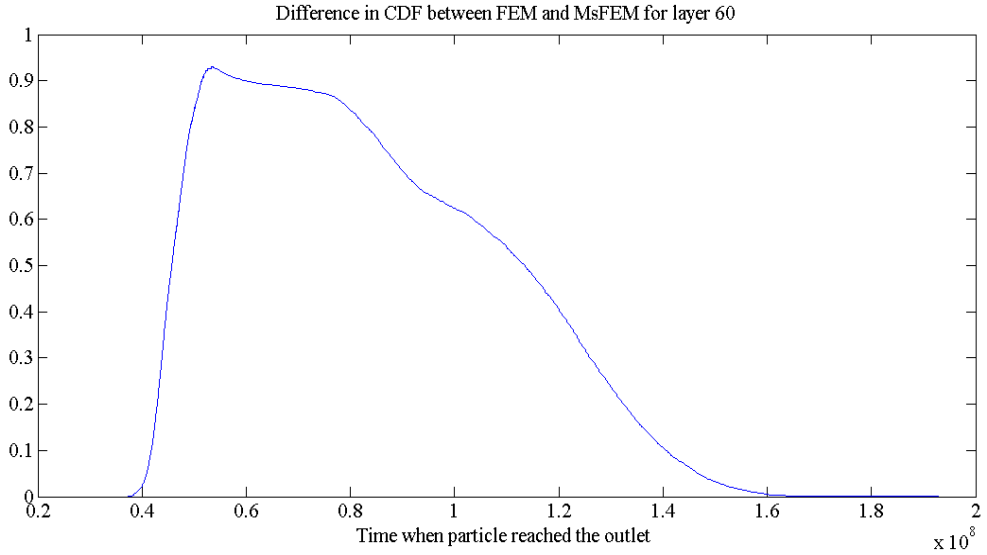

Figure 18: Difference between empirical CDF:s of MsFEM and FEM for layer 60

In figure 19, the empirical probability densities for MsFEM and FEM are shown, but now for layer 60.

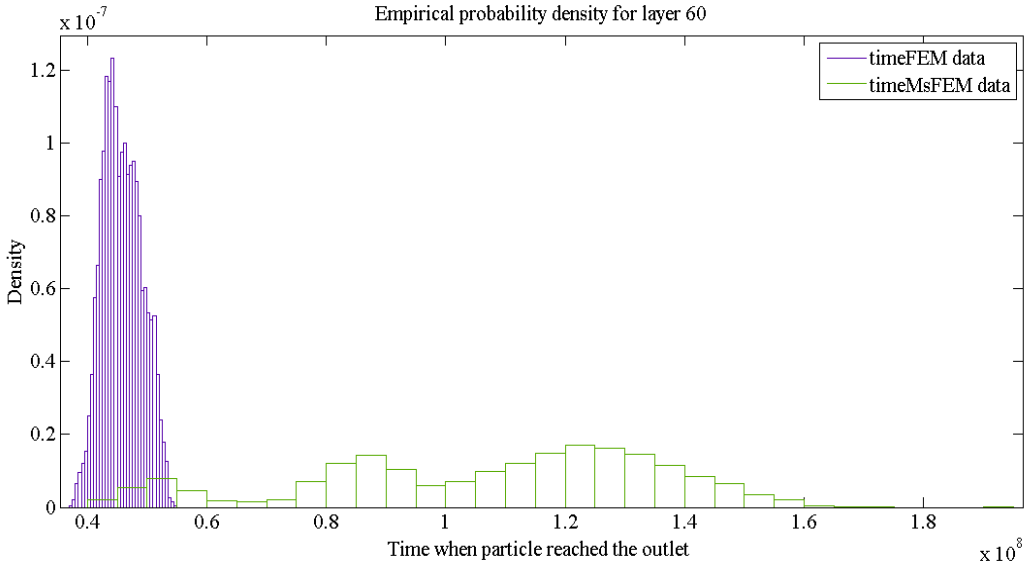

Figure 19: Empirical probability densities for layer 60.

When comparing figure 16 and 19, it's very clear that the displacement, as well as the spreading, is much larger in layer 60 than in layer 1.

In layer 1, the mean time for FEM is $5{,}0789 \cdot 10^4$ time units and the mean time for MsFEM is $6{,}1904 \cdot 10^4$ time units.

In layer 60, the mean time for FEM is $4{,}5836 \cdot 10^7$ time units and the mean time for MsFEM is $1{,}0743 \cdot 10^8$ time units.

This means that the average MsFEM times in layer 1 are displaced with 22% from the average FEM times. In layer 60, however, the displacement is 134%. This, in turn, means that when the permeability contains distinct canals, the MsFEM is much less accurate compared to FEM than in layers where there are no canals. In fact, for many of the permeability layers, the particles didn't even reach the outlet.

5. Conclusions

As can be seen from the results in section 4.1, the multiscale finite element method seems to be able to capture the large scale structure although it has a tendency to reduce the overall pressure. This means that the pressure gradients will decrease, which in turn, through Darcy's law, will lead to a lower velocity. A comparison of the pressure between layers 1 and 60 in section 4.1, shows that the MsFEM pressure field in layer 60 has a much lower overall pressure compared to the FEM solution than it does in layer 1.

The above conclusions are also verified in the results in section 4.3, where the average times have been increased by 22% in layer 1 and 134% in layer 60. As discussed earlier, this stems from the fact that the permeability in layer 60 contains a canal which violates the assumption that the differential operator behaves locally.

A further indication that canals cause the MsFEM to give inaccurate results compared to FEM, can be seen in the relative energy norms, put forward in section 4.2.

6. Discussion

The results in this report indicate that MsFEM, implemented with linear boundary conditions, is able to capture large scale structures. But as soon as the permeability contains a canal, there is reason to doubt that the method gives any valuable results at all. However, we can see that, also for smoother layers, MsFEM fails to capture the small scale features the way FEM does.

It is possible that an improvement can be obtained by changing the boundary conditions for the solution of the macro scale basis functions, so that they take into account the local permeability. But the fact still remains, that when decoupling the problem one fails to account for the non-local behaviour of the differential operator.

A suggestion as how to improve the accuracy of MsFEM, so that it takes into account some of the global information, is put forward by Hou and Efendiev in [5].

In [2], an alternative method is derived, where the size of the local domains are chosen automatically in adaptive algorithm so that the non-local nature of the differential equation is captured. An a posteriori estimate is also presented which guarantees the accuracy of the solution.

7. References

[1] T. Y. Hou and X.-H. Wu, *A multiscale finite element method for elliptic problems in composite materials and porous media*, J. Comput. Phys., 134, (1997), 169-189.

[2] A. Målqvist and Mats G. Larson. *Adaptive variational multiscale methods based on a posteriori error estimation: Energy norm estimates for elliptic problems*, Comput. Methods Appl. Mech. Engrg. 196 (2007) 2313–2324

[3] Axel Målqvist, assistant professor at the Division of Scientific Computing, at the Department of Information Technology, Uppsala University.

[4] Conversation with Axel Målqvist, assistant professor at the Division of Scientific Computing, at the Department of Information Technology, Uppsala University.

[5] Y.Efendiev ans T.Hou, *Multiscale finite element methods for porous media flows and their applications*, Applied numerical mathematics, 2007 – Elsevier

8. Appendix

Table 1: Table over energy norms for 11 different partitions and all layers

	2x2	5x5	5x15	11x10	20x10	22x15	44x15	55x15	55x30	110x30	220x60
Layer 1	0,998505	0,985569	0,99576	0,867539	0,817392	0,79967	0,681847	0,640436	0,557664	0,406726	0
2	1,198093	1,188347	0,949309	1,046197	0,945173	0,790625	0,674661	0,645609	0,534582	0,412944	0
3	1,34935	1,015178	0,948405	0,892292	0,766347	0,746381	0,627764	0,622368	0,528654	0,414628	0
4	1,124709	1,168111	0,973487	0,966594	0,80261	0,734381	0,652663	0,679467	0,601559	0,483569	0
5	1,02433	0,959398	0,919233	0,894049	0,896472	0,783874	0,640006	0,590824	0,528373	0,42638	0
6	1,034983	1,221054	1,005171	0,970608	0,857057	0,856606	0,776784	0,63522	0,559862	0,415935	0
7	1,03143	0,941405	0,918499	0,882537	0,854863	0,805263	0,68372	0,655173	0,566001	0,411036	0
8	1,204669	1,012037	0,992556	0,931231	0,917171	0,81868	0,702087	0,654365	0,61828	0,427306	0
9	1,045273	1,00497	1,017154	0,978696	0,956883	0,953349	0,927706	0,86844	0,696945	0,479544	0
10	1,357998	1,15602	1,026022	0,934977	0,880162	0,877834	0,770015	0,753449	0,644256	0,522899	0
11	1,009327	1,007688	1,00032	0,989618	0,869531	0,859848	0,834731	0,847723	0,795922	0,504742	0
12	1,017756	0,994256	1,003765	0,978378	0,971084	0,958654	0,82274	0,750116	0,671852	0,509902	0
13	1,023189	1,010651	1,041588	0,857158	0,847242	0,856584	0,683491	0,635675	0,502695	0,387076	0
14	1,166413	0,93975	0,907161	0,948293	0,835758	0,816599	0,721566	0,691587	0,652214	0,528356	0
15	1,018697	1,011288	0,996417	0,969328	0,89562	0,884175	0,698995	0,565127	0,517245	0,36863	0
16	0,996897	1,002194	0,985983	0,966002	0,937913	0,884129	0,796695	0,766848	0,665232	0,538018	0
17	1,01483	0,99201	0,957083	0,905363	0,892916	0,857659	0,758142	0,737429	0,664273	0,492795	0
18	1,04321	1,01402	0,979193	0,921019	0,923147	0,888505	0,829781	0,831929	0,69418	0,523813	0
19	1,00584	1,031788	1,085425	0,992178	0,935279	0,868778	0,746981	0,707533	0,624058	0,482413	0
20	0,988762	1,036632	1,094554	0,995	0,892326	0,843856	0,739308	0,760585	0,64487	0,460301	0
21	0,992011	0,969731	0,962883	0,912577	0,893701	0,833432	0,612638	0,61056	0,668867	0,440504	0
22	1,009507	1,005167	0,990871	0,992286	0,952518	0,924579	0,850958	0,818178	0,703776	0,498355	0
23	1,047283	1,074847	1,091912	1,057059	0,894869	0,814458	0,666235	0,608118	0,527242	0,391482	0
24	1,008327	0,936857	0,959575	0,962449	0,784359	0,706448	0,646196	0,611755	0,52923	0,406614	0
25	0,987935	0,942259	0,955379	0,881716	0,766998	0,759439	0,691079	0,656021	0,578587	0,466217	0
26	0,997025	1,048909	1,017394	1,042951	0,912169	0,855819	0,767192	0,729832	0,639588	0,504395	0
27	0,992305	1,002154	0,983701	1,016379	0,920489	0,871078	0,7492	0,775937	0,740739	0,596269	0
28	0,934151	0,864876	0,818961	0,809529	0,718875	0,700771	0,618288	0,596137	0,508632	0,404274	0
29	0,96201	1,075202	1,003409	0,887327	0,801699	0,750188	0,590435	0,594118	0,507466	0,377292	0
30	0,992695	1,026468	1,000607	0,963327	0,902585	0,891007	0,807223	0,787827	0,713286	0,529231	0

31	0,999013	0,949963	0,916443	0,907515	0,795489	0,740877	0,67803	0,616669	0,535759	0,38107	0
32	1,002102	0,986649	0,984519	0,929254	0,80553	0,786927	0,784981	0,741307	0,645661	0,433993	0
33	0,99605	0,990071	0,985447	0,973204	0,934889	0,892659	0,775496	0,775461	0,695983	0,546302	0
34	1,006537	0,984098	0,986291	0,914436	0,869486	0,895757	0,787924	0,806201	0,672976	0,49121	0
35	1,000884	1,0363	1,020008	0,915316	0,840169	0,806678	0,744347	0,696465	0,6089	0,504902	0
36	1,028657	1,65729	1,069728	2,167721	2,490443	1,238796	1,218786	2,179944	3,376672	2,256754	0
37	1,003653	1,251476	1,211747	1,639173	2,316015	2,468119	1,999679	2,693723	2,737186	7,921775	0
38	1,011759	1,973751	2,14061	2,435883	2,462662	3,140626	2,739066	3,893155	1,514959	1,56599	0
39	1,387967	1,72922	1,225034	1,107212	1,61768	1,421786	1,364487	1,121068	0,921637	0,709971	0
40	1,27234	1,988535	1,450942	2,247475	4,245979	1,60017	4,259405	2,099331	1,953366	1,106235	0
41	2,419085	1,825615	1,640247	2,658652	4,869435	3,56555	3,933791	2,80279	1,438994	1,636902	0
42	3,515638	1,050284	0,989175	1,639931	3,802208	2,50769	2,337514	1,76175	2,958788	0,939696	0
43	1,259871	1,07093	1,027495	0,985033	0,936025	0,914701	2,133951	3,333374	3,686835	0,997116	0
44	1,006096	1,021971	1,00323	1,002386	1,024313	0,823624	0,934837	0,922678	1,005018	0,839477	0
45	1,003553	1,040879	1,006506	1,000176	1,539943	0,763324	0,804974	0,703593	0,612304	0,751734	0
46	1,0073	1,074724	1,005185	1,004371	1,138381	0,860487	0,816571	0,830594	0,73619	0,903854	0
47	1,019536	1,449093	1,011579	1,71767	2,327925	1,166577	1,051586	0,979846	1,066579	0,712267	0
48	2,667896	1,883668	1,130221	3,142018	2,984182	1,685734	1,164638	1,116137	0,90038	0,689602	0
49	1,03402	3,864023	1,053862	1,107641	0,874613	2,017979	1,259638	1,046187	1,970543	1,018154	0
50	1,055751	1,027802	3,45235	14,12336	5,759788	7,586179	13,78414	14,26901	1,874158	12,96749	0
51	1,715558	1,110123	1,043918	2,337137	1,206315	1,80125	1,395537	1,268161	1,325358	1,076027	0
52	1,14539	1,647421	1,175742	1,518088	1,35476	1,350926	1,148878	1,212591	0,946925	1,006527	0
53	0,930286	1,011335	0,979039	1,446759	1,249727	1,223971	1,043674	0,933624	0,860202	0,756037	0
54	1,008808	1,053792	1,016272	2,043159	1,250611	1,216048	1,229523	1,973309	1,019448	1,152085	0
55	1,001095	1,002233	1,000542	1,001034	1,001869	1,00404	10,82927	11,88709	0,880411	24,09518	0
56	1,036647	1,096597	1,033509	1,048458	1,04933	0,961164	1,010435	1,054216	0,918933	0,785373	0
57	0,971564	1,036973	1,027032	1,110802	1,095944	1,073527	0,9706	1,004997	1,024978	0,816898	0
58	1,000598	1,00318	1,00069	1,008131	1,002646	0,985354	1,15041	1,212069	1,25287	0,693538	0
59	0,999848	1,005077	1,000134	1,002215	1,119448	1,251286	4,036101	5,183284	11,38629	17,887	0
60	1,000496	1,017095	1,001723	1,053516	1,345631	1,127572	7,478895	9,180771	19,22731	14,07943	0
61	1,000432	1,011306	1,000869	1,061183	1,01464	1,017552	2,896043	3,70628	8,536805	8,365728	0
62	1,002175	1,001909	1,00072	1,015364	1,015028	1,011099	4,208891	3,577619	9,793787	11,833	0
63	1,002097	1,004838	1,006179	1,021246	0,999766	1,040789	1,847678	12,74301	12,72355	8,133762	0
64	1,001091	1,009984	1,002732	1,118453	3,543501	3,546878	4,261641	5,83593	2,277204	1,70913	0
65	1,002232	1,04031	1,051576	2,130729	2,209579	3,172261	1,399883	2,569393	1,113541	0,966286	0
66	1,036944	1,00408	0,990542	1,465895	1,18129	1,395242	1,851649	2,003495	4,343136	3,453857	0
67	1,001939	0,983062	0,987144	2,457134	1,450648	7,294633	4,587447	3,792298	5,74155	5,192079	0
68	1,005437	3,146179	1,771704	1,244632	1,941498	2,780859	2,567841	4,051558	6,701941	3,774676	0

69	1,002278	1,089256	1,076618	1,278744	3,895048	1,144092	1,948337	2,204084	1,638	1,290134	0
70	1,004239	1,169285	1,176144	2,276849	3,010409	4,980006	7,749085	6,365148	1,314235	1,780144	0
71	1,004928	1,176055	1,429995	2,062929	4,051393	5,582799	10,16701	10,24352	8,442136	6,64823	0
72	1,000404	1,023968	1,038162	1,355517	3,363682	3,728245	2,724858	1,643138	3,060496	1,001221	0
73	1,002224	1,135973	1,018608	1,211577	1,736844	2,234233	1,864254	1,72779	1,251346	1,22032	0
74	1,003683	1,105255	1,194934	1,635135	1,649103	2,278639	2,196421	1,318841	1,65093	0,834025	0
75	1,041936	2,130576	1,860138	2,475098	5,243521	5,116363	6,112343	0,926949	5,029893	0,827445	0
76	1,010646	2,195472	2,719465	3,089199	3,148407	3,524408	2,936292	2,999989	1,193169	1,229505	0
77	1,001211	1,715574	0,984111	1,365396	1,259515	2,054873	1,255573	1,205367	1,204792	0,893106	0
78	1,018707	1,305757	1,035555	2,158972	3,655674	0,925767	0,910246	0,862736	0,849164	2,395351	0
79	1,014716	0,980118	0,989235	7,282143	13,56066	0,920896	0,950794	0,884734	0,867593	9,732281	0
80	1,001003	1,002328	1,023531	2,104175	3,760004	0,951703	0,894372	0,838569	0,872925	4,003899	0
81	1,003109	1,003387	1,069965	4,405932	7,959638	0,957936	0,996248	0,926761	1,484509	9,308635	0
82	1,013566	1,063282	1,033692	1,533441	1,377204	1,111778	1,170054	1,093206	0,929941	0,761276	0
83	1,986888	1,034569	0,948907	1,080357	0,968312	1,003194	0,986296	0,928761	0,825316	0,735012	0
84	1,096135	1,041442	0,983641	1,068548	1,052856	1,123919	1,034433	1,04713	0,905454	0,786734	0
85	0,942975	1,00513	0,96626	1,043571	0,963126	1,017881	0,918109	0,927901	1,00902	0,658688	0